Title: Gestational LSD exposure in mouse rapidly reaches embryonic CSF and is associated with altered choroid plexus signaling, cerebral cortical development, and offspring behavior

Authors: Ya'el Courtney[1,2], Josephine M. Anderson[3], Christian Lagares-Linares[1,2], Cody J. Wenthur[3,4], Maria K. Lehtinen[1,2]*

Affiliations:

[1] Department of Pathology, Boston Children's Hospital and Harvard Medical School; Boston, MA, USA.

[2] Program in Neuroscience, Harvard Medical School; Boston, MA, USA.

[3] School of Pharmacy, University of Wisconsin; Madison, WI, USA.

[4] Transdisciplinary Center for Research in Psychoactive Substances, University of Wisconsin; Madison, WI, USA.

*Corresponding author. Email: maria.lehtinen@childrens.harvard.edu

Abstract: Classic serotonergic psychedelics engage 5-HT receptors throughout the nervous system, but how maternal exposure intersects with embryonic brain interfaces is poorly defined. Here we tested in mice whether maternally administered lysergic acid diethylamide (LSD) accesses embryonic cerebrospinal fluid (CSF) and whether embryonic choroid plexus (ChP) – a CSF-secreting epithelium enriched for *Htr2c* – mounts an acute response. Following a single maternal injection (0.3 mg kg^{-1}, subcutaneous), LSD was detectable in embryonic CSF within 5–15 minutes at E12.5 and E16.5. Thirty minutes after maternal dosing, LSD induced Fos in embryonic ChP across ventricles and was accompanied by rapid apical remodeling and increased embryonic CSF protein. In parallel cohorts, psilocybin, 5-MeO-DMT, and the 5-HT_2C agonist WAY-161503 elicited a similar Fos response in ChP. Prenatal LSD exposure during mid-gestation was associated with altered S1 cortical cellularity and projection-neuron subtype marker composition at P8; regimen-dependent effects included male-biased changes in $SATB2^+$ and $CTIP2^+$ populations after repeated exposure. In adulthood, offspring exhibited modest, male-predominant reductions in prepulse inhibition and increased rotational stereotypy. Together, these data identify embryonic CSF as a rapidly accessible compartment for maternal LSD and support a model in which serotonergic agonists can acutely engage ChP epithelium during cerebral cortical development.

34 **Significance:** Psychedelic use during pregnancy is increasing, but the speed and extent to which
35 these drugs access the embryonic CNS remain unknown. We show that a single maternal dose of
36 LSD appears in mouse embryonic cerebrospinal fluid within five minutes and provokes an
37 immediate response in the choroid plexus, a serotonin receptor-rich epithelium that regulates CSF
38 composition. Psilocybin, 5-MeO-DMT, and a selective 5-HT_2C agonist trigger a similar response.
39 Mid-gestational exposure alters cortical neuron composition in neonates and produces persistent
40 behavioral abnormalities in adult offspring, including stereotypies evident from weaning. These
41 data reveal that maternal serotonergic agonists rapidly access embryonic CSF, acutely activate
42 choroid plexus epithelium, and are associated with lasting changes in cortical composition and
43 offspring behavior.

44

45

46 **Main Text:**

47 Serotonin shapes neural proliferation, migration, and circuit assembly across embryonic
48 and early postnatal development (Gaspar et al., 2003; Bonnin et al., 2011; Shah et al., 2018;
49 Carvajal-Oliveros and Campusano, 2021). Exogenous serotonergic agonists administered during
50 gestation therefore have the potential to engage developmental programs, but the routes by which
51 maternal compounds access embryonic brain compartments - and which embryonic interfaces
52 respond acutely - remain incompletely defined. A key unresolved question is whether maternally
53 administered serotonergic psychedelics reach embryonic cerebrospinal fluid (CSF), where they
54 could interact with CSF-contacting target cells during cerebral cortical neurogenesis.

55 One candidate target interface is the choroid plexus (ChP). The ChP is a secretory
56 epithelium that produces CSF (Damkier et al., 2013; Lun et al., 2015; MacAulay et al., 2022) and
57 helps shape the molecular environment of the developing brain (Saunders et al., 2023).
58 Transcriptomic atlases indicate that *Htr2c* is prominently expressed in ChP epithelium relative to
59 other serotonin receptor subtypes (Dani et al., 2021), and early autoradiographic work showed that
60 ^{125}I-LSD binds serotonergic sites on ChP epithelial cells at a density ten-fold higher than any other
61 serotonergic site in brain homogenates (Yagaloff and Hartig, 1985). Functionally, cultured ChP
62 epithelial cells mount immediate-early gene responses to serotonergic hallucinogens (Sanders-
63 Bush and Breeding, 1991). In parallel, CSF-borne cues influence cerebral cortical development
64 (Gato and Desmond, 2009; Lehtinen et al., 2011; Fame and Lehtinen, 2020), raising the possibility
65 that acute drug-evoked changes in ChP state could modulate developmental signaling via CSF.

66 We focused on LSD as a prototypical, high-potency serotonergic psychedelic with well-
67 characterized receptor pharmacology and extensive rodent behavioral and pharmacokinetic data,

68 which facilitated sensitive quantification from the small volumes of embryonic CSF. To test
69 whether ChP activation is specific to LSD versus a broader feature of serotonergic agonism, we
70 additionally compared acute ChP Fos responses following maternal exposure to psilocybin, 5-
71 MeO-DMT, and the selective 5-HT_2C agonist WAY-161503.

72 Here we asked three questions. First, does maternally administered LSD rapidly access
73 embryonic CSF during mid-gestation? Second, does the embryonic ChP mount an acute
74 transcriptional and structural response consistent with serotonergic receptor engagement? Third,
75 are mid-gestational exposure regimens associated with changes in early postnatal cerebral cortical
76 cellular organization and adult behavioral readouts in offspring? We combine LC–MS/MS
77 pharmacokinetics with embryonic CSF sampling, ChP immediate-early gene and epithelial
78 remodeling assays, and analyses of cortical marker composition and behavior. Our data support an
79 interface-focused model for how maternal serotonergic agonists can engage the developing brain.

80 **Materials and Methods**

81 See Supplemental Methods for a complete description of experimental methods as well as detailed
82 information about all resources used and material associated with this article.

83 *Ethical approval.* All procedures complied with institutional and national guidelines. Animal work
84 was approved by the Boston Children's Hospital IACUC.

85 *Animals.* Adult and timed-pregnant CD-1 mice (Charles River; Jackson Laboratory; or in-house
86 colonies) were maintained at 21 ± 1.5 °C, 35–70% humidity, 12-h light/dark with ad libitum
87 food/water. Unless stated, experiments used equal numbers of males and females. Sample sizes,

88 sex, and ages are provided in figure legends. Litter was tracked and used as a factor in sensitivity
89 analyses.

90 *Drugs and dosing (in vivo).* Timed-pregnant dams received subcutaneous injections in sterile 0.9%
91 saline: WAY-161503 3 mg kg^{-1} (Tocris, Cat. 1801); (+)-lysergic acid diethylamide tartrate (LSD)
92 0.3 mg kg^{-1} (NIDA Drug Supply Program); psilocybin 3 mg kg^{-1} (NIDA); 5-MeO-DMT 50 mg
93 kg^{-1} (NIDA). Solutions: WAY-161503, 10 mM at 1 μL g^{-1}; LSD tartrate, 0.6 mM at 0.6 μL g^{-1};
94 psilocybin from a 15.03 mg mL^{-1} stock at 0.1995 μL g^{-1} (saline added to a minimum 50 μL total);
95 5-MeO-DMT, 50 mg mL^{-1} at 1 μL g^{-1}. Body weight and injection/sacrifice times were logged for
96 PK.

97 *Choroid plexus (ChP) dissections.* Lateral ventricle (LV), third ventricle (3V), and fourth ventricle
98 (4V) ChP were microdissected using standard landmarks. LV ChP was exposed by hippocampal
99 reflection; adult 3V ChP was visualized along the dorsal midline; 4V ChP was accessed via
100 cisterna magna exposure.

101 *Behavioral testing.* Behavior was performed with the BCH Animal Behavior & Physiology Core
102 (blinded, randomized; litter-balanced where possible). Open-field test: Adult CD-1 mice (n=10 per
103 condition unless noted) explored a 40×40 cm arena for 15 min. Primary outcomes were total
104 distance traveled and rotational stereotypy**;** spatial occupancy metrics (e.g., centroid/heatmaps)
105 were used as descriptive visualizations. Rotations were quantified from the animal's instantaneous
106 heading angle relative to the arena center. A "rotation" was defined as ≥360° cumulative angular
107 displacement in a single direction, with direction determined by the sign of angular velocity.
108 Prepulse inhibition: Background 60 dB, pre-pulses 70/74/78/82 dB (20 ms), startle 105 dB (40

109 ms), 100 ms ISI, 10–30 s randomized ITI. %PPI = 100 × [(pulse-alone – (prepulse+pulse))/pulse-
110 alone].

111 *Immunostaining and imaging*. Explants: ChP explants fixed (4% PFA, 10 min), permeabilized
112 (0.1% Triton X-100), primary overnight at 4 °C, secondary 2 h at room temperature; Hoechst
113 33342 counterstain; Fluoromount-G mounting. Sections: Postnatal brains perfused with PBS then
114 4% PFA, cryoprotected (10%→20%→30% sucrose), embedded in OCT, permeabilized, and
115 stained as above. Confocal imaging on Zeiss LSM710/980 (20× air; 63× oil). Acquisition in ZEN
116 Black; Airyscan processing in ZEN Blue when specified**.**

117 *Image quantification.* Aposomes: Four 20× fields per explant were scored by a blinded rater; the
118 mean per explant constituted N=1. FOS+ nuclei: Four 20× fields per explant were thresholded in
119 FIJI; Analyze Particles counted FOS and DAPI objects (>200 px). Proportion FOS+ = FOS/DAPI;
120 field means per explant constituted N=1. Cortical marker classes: SATB2/CTIP2/TBR1 images
121 spanning S1 cortex (L1 to corpus callosum) were exported as 4-channel TIFFs and analyzed in
122 Biodock (trained model; QC-checked). Cells were binned into six equal depth bins (y-axis). Class
123 frequencies per bin were exported to R for summaries and to GraphPad Prism for plotting.

124 *Real-time quantitative PCR (RT-qPCR).* ChP was microdissected, snap-frozen, and total RNA
125 extracted (NEB Monarch Total RNA kit). 100 ng RNA was reverse-transcribed (NEB LunaScript).
126 qPCR used TaqMan Gene Expression Master Mix (Thermo Fisher) with Mm00487425_m1 (Fos)
127 and Hs99999901_s1 (18S) on a Roche LightCycler 480II. Cycling: 95 °C 10 min; 40×(95 °C 15
128 s/60 °C 1 min). Triplicates were run. Relative expression used 2^–ΔΔCT (normalized to 18S).

129 *Whole-mount clearing and light-sheet imaging.* E12.5 heads were fixed in 4% PFA, processed
130 with SHIELD (LifeCanvas; small-sample workflow), delipidated in SDS buffer at 45 °C,

131 immunolabeled for c-FOS, index-matched in EasyIndex, and imaged on a Zeiss Lightsheet 7 (5×
132 objective). Z-stacks were stitched in ZEN; 16-bit TIFFs were volume-rendered in syGlass v2.3.0
133 with identical linear transfer functions.

134 *Pharmacokinetics Analysis via LC–MS/MS.* Serum and CSF samples were analyzed using a Sciex
135 QTrap 5500 coupled to a Waters ACQUITY UPLC I-Class. LSD and d3-LSD (ISTD) were
136 quantified using quadratic standard curves, 1/x^2 weighting; calibrators retained if ≥85%
137 (R^2≥0.995). Mobile phases were water (A) and acetonitrile (B) with 0.1% Formic Acid, run a
138 0.375mls/min through a Phenomenex Kinetex Phenyl-Hexyl (1.7um, 100x1.2mm) held at 35 °C.
139 Gradient: 5–40% B to 1.75 min; 95% B to 2.5 min; re-equilibrate to 3.0 min. Analytes were
140 monitored in MRM mode (positive) via the following unique transitions; (324.162>223.00,
141 209.10, 207.10) and d3-LSD (327.160> 226.10, 208.00, 180.10). Calibrators were generated using
142 blank CD1 mouse serum and artificial CSF (aCSF). Samples were prepared via a Waters Sirocco
143 Protein Precipitation Plates. Injections were submitted in triplicate in randomized sets of 6 with a
144 blank between each injection.

145 *Quantification and statistical analysis*. Analyses were pre-planned, randomized, and blinded
146 where possible. Power analyses (α=0.05, 1–β=0.80) informed group sizes using pilot variance.
147 Outliers: ROUT (Q=1%). Normality (Shapiro–Wilk) and variance homogeneity (F-test/Bartlett)
148 guided test selection. Parametric: unpaired t-test (Welch if unequal variances); one-way ANOVA
149 (Tukey) for ≥3 groups; two-way ANOVA (Sidak) for two factors. Nonparametric: Mann–Whitney
150 U; Kruskal–Wallis (Dunn). Sex was included where relevant; litter evaluated as a random intercept
151 in sensitivity models. Data are mean ± SD (or mean ± SEM for multiple measures per animal).
152 Exact n, tests, and P values are reported in legends.

153 **Results**

154 **Maternal LSD rapidly reaches embryonic CSF in mouse**

155 We tested and found that maternally administered LSD crosses the placenta and reaches
156 the embryo by measuring drug levels in maternal serum, embryonic serum (E16.5), and embryonic
157 CSF at E12.5 and E16.5 following a single subcutaneous dose of 0.3 mg kg^{-1}; samples were
158 collected at 5, 15, 30, 60, and 120 min (**Fig. 1A**). Doses were selected to ensure target engagement
159 in mouse and are not human-equivalent. Maternal serum was obtained via cardiac puncture. At
160 E16.5, embryonic serum was collected by venipuncture of a cervical vein under stereomicroscopic
161 guidance using a pulled glass microcapillary pipette. Embryonic CSF was collected at E12.5 and
162 E16.5 from the cisterna magna using a glass microcapillary pipette under stereomicroscopic
163 guidance, as previously described (Zappaterra et al., 2013), minimizing blood or neuroepithelial
164 contamination.

165 We developed a small-volume LC–MS/MS assay for mouse serum and embryonic CSF
166 using d3-LSD as the internal standard. Calibration curves were prepared in-matrix (blank serum
167 or artificial CSF), were linear across the working range (R^2 ≈0.997), and supported a lower limit
168 of quantitation of 0.25 ng mL^{-1}. Calibration curves prepared in-matrix met acceptance criteria,
169 with back-calculated bias within −8% to +9% (serum) and −8% to +8% (CSF) and replicate CV ≤
170 2.7% both matrices (**Fig. 1B–C**).

171 Following a single maternal dose of 0.3 mg kg^{-1}, maternal serum reached its highest
172 concentration at 5 min (419.6 ng mL^{-1}) and then declined with an elimination half-life of ≈39.0
173 min based on the 30–120 min log-linear phase (**Fig. 1D**). At E16.5, embryonic serum peaked at 5
174 min (≈107.8 ng mL^{-1}; ~26% of the maternal maximum) and showed a half-life of ≈53.0 min by

175 the same approach (**Fig. 1E**). Embryonic CSF contained measurable LSD by 5–15 min at both
176 ages, with 15-min peaks of ≈15.2 ng mL^{-1} (E12.5; $t_{1/2}$ ≈64.9 min) and ≈28.4 ng mL^{-1} (E16.5; $t_{1/2}$
177 ≈52.5 min), remaining above the assay limit at 120 min (≈1.8 and 1.6 ng mL^{-1}, respectively) (**Fig.**
178 **1F**). At 15 min, CSF levels at E16.5 were ~1.9× those at E12.5 and were ~50% of the paired
179 embryonic-serum concentration. Across 0–120 min, total embryonic-serum exposure was ~17%
180 of maternal serum, and CSF exposure at E16.5 exceeded E12.5 by ~1.4×. Taken together, these
181 data demonstrate that LSD crosses the placenta and reaches the embryonic CSF within minutes.
182

183 **Prenatal LSD reshapes S1 neuron composition and microglia at P8**

184 Maternal LSD exposure was associated with regimen-dependent changes in S1 cortical
185 cellularity and projection-neuron subtype marker composition at P8 (**Fig. 2**). The experimental
186 design (**Fig. 2A**) contrasted a single 0.3 mg kg^{-1} injection at E12.5 ("acute") with the same dose
187 given once daily from E12.5-E16.5 ("repeated"). At the 0.3 mg kg^{-1} dose, no adverse events such
188 as maternal weight loss, altered grooming, or changes in pup retrieval were observed. Litter size,
189 pup viability, birth weight, brain weight, and brain-to-body ratio at birth did not differ between
190 LSD-exposed and control litters (**Fig. S1A-D**). Brains were examined at postnatal day 8 (P8), when
191 laminar identities and glial profiles are well resolved but before extensive synaptic pruning.

192 Across six equal-width bins spanning pia to white matter, $DAPI^{+}$ nuclei were reduced
193 following LSD (two-way ANOVA, Treatment effect $P < 0.0001$; **Fig. 2B**). Acute exposure
194 produced the larger deficit, 1,090-2,020 cells mm^{-2} (21–49 % below control, post hoc $P \leq 0.0008$
195 in every bin), whereas repeated exposure reduced nuclei by 580 – 1,260 cells mm^{-2} (16–40 %;
196 $P \leq 0.027$). A Treatment × Sex interaction was not detected for total nuclei ($F_{2,168} = 0.34$, $P = 0.71$),
197 indicating a comparable global loss in males and females.

198 SATB2, CTIP2, and TBR1 are transcription factors commonly used to operationalize
199 major cortical projection-neuron subclasses during early postnatal development, and we used these
200 markers as indices of subclass composition. Cerebral cortical layer marker quantification revealed
201 shifts among corticofugal/subcerebral ($CTIP2^+$), callosal ($SATB2^+$) and corticothalamic ($TBR1^+$)
202 neurons (**Fig. 2C-E**). Repeated dosing increased the $CTIP2^+$ fraction from 19.7 ± 1.5 % to
203 28.1 ± 1.9 % (difference +8.4 percentage points [pp], one-way ANOVA with Dunnett's multiple
204 comparisons $P = 0.026$), whereas acute dosing did not change $CTIP2^+$ abundance. $SATB2^+$
205 neurons were selectively vulnerable, dropping by 13.6 pp with repeated exposure
206 (46.5 ± 1.6 % → 32.9 ± 2.1 %, $P < 0.0001$) and by 22.9 pp after acute exposure (to 23.7 ± 1.7 %,
207 $P < 0.0001$). $TBR1^+$ neurons declined under both regimens (–12.8 pp repeated, –16.1 pp acute;
208 $P \leq 0.0005$). The "DAPI-only" fraction (nuclei lacking these three markers) rose by 9.7 pp with
209 repeated LSD ($P = 0.023$) and by 15.4 pp with acute LSD ($P = 0.0002$).

210 Stratifying by sex and cortical depth (**Fig. 2F–N**) revealed a significant
211 Treatment × Sex × Bin interaction for $CTIP2^+$ and $SATB2^+$ populations ($F_{10,250} = 3.21$,
212 $P = 0.0007$). In males, repeated LSD reduced $SATB2^+$ neurons in bins 1–5 by 28–52 % (all
213 $P \leq 0.040$) and doubled $CTIP2^+$ neurons in bin 2 (+20.5 pp, $P = 0.0042$), with smaller gains in
214 bin 5. Females showed no detectable $CTIP2^+$/$SATB2^+$ shifts. $TBR1^+$ loss was equivalent across
215 sexes and confined to deep bins 5–6 (–19 – 22 pp; $P < 0.0001$). Acute exposure produced parallel
216 $SATB2^+$ and $TBR1^+$ deficits in both sexes without altering $CTIP2^+$ levels.

217 $IBA1^+$ microglia density increased with repeated dosing from 166.8 ± 6.2 to
218 204.5 ± 8.3 cells mm^{-2} (+22 %, Dunnett post hoc $P = 0.0036$, **Fig. S1E**) and rose modestly after
219 acute dosing (192.6 ± 9.8 cells mm^{-2}, +16 %, $P = 0.044$, **Fig. S1F**). GFAP staining revealed

220 reactive astrocytic rims surrounding ectopic parvalbumin-positive interneuron clusters posterior to
221 the anterior commissure, which only appeared in LSD-exposed mice (**Fig. S1G**).

222 In sum, prenatal LSD exposure was associated with reduced S1 cellularity at P8 and altered
223 composition of projection-neuron subtype marker populations. Both exposure regimens reduced
224 SATB2^{+} and TBR1^{+} populations, while repeated exposure was additionally associated with
225 increased CTIP2^{+} fractions in males and elevated microglial density. These data define regimen-
226 and sex-contingent early postnatal cortical signatures following mid-gestational serotonergic
227 exposure.
228

229 **Prenatal LSD exposure is associated with reduced sensorimotor gating (PPI) and increased**
230 **rotational stereotypy**

231 To test for lasting behavioral effects following in utero LSD exposure, we evaluated
232 offspring at P90 on prepulse inhibition of acoustic startle (PPI, **Fig. 3A**) and open-field behavior.
233 Pregnant mice received either one single LSD injection at E12.5 (acute) or daily injections from
234 E12.5 to E16.5 (repeated), with repeated saline-treated dams as controls (**Fig. 3B**).

235 When sexes were combined, PPI was reduced after prenatal LSD (**Fig. 3C**). In sex-
236 stratified analyses, males showed reduced PPI following repeated exposure (**Fig. 3D**), whereas
237 females did not differ at the group level at this N despite clear individual variability (**Fig. 3E**).
238 Startle amplitude was higher in females in both LSD conditions across intensities (**Fig. 3H**), and
239 in males differed only for the repeated group at the highest intensity (**Fig. 3G**). Startle latency
240 showed no consistent group effect. The only reliable change was a slower response at 82 dB in
241 acute LSD females (**Fig. S2A-C**). These patterns indicate that amplitude changes do not account
242 for the PPI reduction, which was most robust in males.

243 Open field revealed a stereotypy-dominant phenotype rather than gross hyperactivity.
244 Representative single-mouse occupancy heatmaps are shown in **Fig. 3I**, with group-mean
245 occupancy heatmaps in **Fig. 3J**. Total rotations were increased following prenatal LSD (negative-
246 binomial GLM, Group LR χ^2=8.02, P=0.018; back-transformed means ±SE: control 54.2 ±12.6,
247 acute 136.2 ±31.3, repeated 81.4 ±18.8; Tukey control vs acute P=0.013; **Fig. 3K**). Using a control-
248 anchored threshold (95th percentile of control), "high-rotators" were more frequent in LSD groups
249 (acute 2/10, repeated 4/10, control 1/10; **Fig. 3L**). Spatial organization shifted without large
250 changes in distance or velocity, as observed in pooled centroid distributions (**Fig. 3M**) and in the
251 full set of raw path traces (**Fig. S2E**). Direction-specific rotation counts are provided in **Fig. S2F**.

252 Attempts to assess higher-order behaviors, including novel object recognition and social
253 approach, were confounded by elevated baseline stereotypy and abnormal exploration, rendering
254 these assays uninterpretable. Beginning at P21 and persisting through at least P156, 7 of 10 mice
255 with repeated exposure and 5 of 10 with acute exposure exhibited continuous stereotypies
256 (backflipping, tight circling, upright corner-hopping). At P156, females had lower body weight
257 following repeated exposure (35.3 vs 43.7 g, P=0.021) and higher brain mass after acute exposure
258 (0.635 vs 0.550 g, P=0.0001); males did not differ, and the acute female brain-mass effect
259 remained significant after adjusting for body weight (**Fig. S3A-H**). Testis mass was unchanged;
260 the testis-to-body ratio was higher after acute exposure (P=0.021). A blinded midline screen of
261 atlas-matched coronal sections at P156 identified ventriculomegaly with frontal-horn
262 predominance in LSD groups (control 1/10, acute 9/10, repeated 8/10; **Fig. S3I**) and rarer callosal
263 variants, including asymmetric hypoplasia, an occasional supracallosal diverticulum continuous
264 with the frontal horn, and partial agenesis of the anterior corpus callosum; given limited atlas levels
265 and modest N, these reads are descriptive.

266 Overall, prenatal LSD exposure was associated with adult behavioral differences that were
267 most robust in male offspring after repeated exposure (reduced PPI) and across groups as increased
268 rotational stereotypy. Effect sizes for PPI were modest, and several higher-order assays were not
269 interpretable due to elevated baseline stereotypy, which we therefore report as an important
270 phenotype in its own right. Because we did not test persistence of the P8 cortical marker
271 differences into adulthood or manipulate candidate receptors, we treat links between early cortical
272 signatures and adult behavior as hypotheses motivated by the timing of embryonic exposure and
273 the observed developmental phenotypes.

274 **Maternal serotonergic agonists activate embryonic choroid plexus and change CSF**

275 Given the rapid appearance of LSD in embryonic CSF, we asked whether the embryonic
276 ChP mounts an acute response to maternal serotonergic agonists. We quantified Fos induction after
277 maternal dosing with LSD (0.3 mg kg^{-1}), psilocybin (3 mg kg^{-1}), 5-MeO-DMT (50 mg kg^{-1}), or
278 the selective 5-HT_2C agonist WAY-161503 (3 mg kg^{-1}). In separate cohorts, we quantified
279 epithelial apical remodeling and embryonic CSF protein after maternal dosing with LSD and the
280 serotonergic psychedelics psilocybin and 5-MeO-DMT (**Fig. 4**).

281 A single maternal dose of LSD at E12.5 or E16.5 induced rapid activation of ChP
282 epithelium across ventricles. The immediate early gene *Fos* was upregulated within 30 min, as
283 measured by qPCR from microdissected ChP collected 30 min after dosing in adult dams (LV
284 ChP) and in E16.5 embryos (LV/3V/4V ChP and brainstem; **Fig. 4C–G**) and by c-FOS
285 immunostaining (**Fig. 4B,H**). The response generalized to WAY-161503, 5-MeO-DMT, and
286 psilocybin (**Fig. 4D–F,G**). Whole-head light-sheet imaging of optically cleared E12.5 embryos
287 further confirmed robust c-FOS in 4V ChP with detectable, but less intense signal in LV ChP (**Fig.**

288 **4L, Fig. S4A-F**). Additional FOS signal was observed in the locus coeruleus in these datasets
289 (anatomical observation; not quantified; **Fig. S4G–H**).

290 Downstream of transcriptional activation, ChP cells showed rapid apical remodeling.
291 Within 30 min of maternal LSD, psilocybin, or 5-MeO-DMT, epithelial cells exhibited increased
292 aposome formation (actin-rich, secretory protrusions [phalloidin/ezrin]), consistent with an
293 apocrine-like secretory state (Courtney and Lehtinen, 2025; Courtney et al., 2025) (**Fig.**
294 **4B,I,L,M**). Functionally, total protein concentration rose in embryonic CSF 30 min following
295 maternal psychedelics at both E12.5 and E16.5 (**Fig. 4J–K**). Together, these data support that
296 maternal psychedelic exposure activates embryonic ChP leading to rapid transcriptional,
297 cytoskeletal, and secretory responses that alter CSF composition.

298 **Discussion**

299 Maternally administered LSD rapidly reached embryonic CSF during mid-gestation and
300 coincided with an acute response in embryonic ChP epithelium, including Fos induction, apical
301 remodeling, and increased CSF protein. In separate cohorts, prenatal exposure during E12.5–E16.5
302 was associated with altered S1 cellularity and projection-neuron subtype marker composition at
303 P8, and with adult behavioral differences most evident as increased rotational stereotypy and
304 modest, male-predominant reductions in prepulse inhibition after repeated exposure. Together,
305 these findings position the embryonic CSF–choroid plexus interface as a rapidly engaged
306 compartment through which maternal serotonergic agonists can access and influence embryonic
307 signaling environments.

308 A key implication of the pharmacokinetic data is that embryonic CSF exposure occurs on
309 a timescale compatible with acute epithelial and neural responses. The ChP is well-positioned to

310 respond to CSF-borne ligands, and transcriptomic atlases and prior *in vitro* work suggest
311 serotonergic responsiveness in ChP epithelium, including prominent *Htr2c* expression. Consistent
312 with this, we observed rapid Fos induction across ventricles after maternal dosing with LSD and
313 with other serotonergic agonists, including a selective 5-HT_2C agonist. We interpret these data as
314 supporting a model in which serotonergic agonists can acutely engage ChP epithelium during
315 development. However, our study did not test receptor necessity. LSD binds serotonergic sites
316 across multiple brain regions, though ChP epithelium harbors the highest reported site density
317 (Yagaloff and Hartig, 1985); resolving the relative contributions of ChP-mediated versus direct
318 neural actions, including at 5-HT_2A-expressing neuronal populations, and potential effects of
319 active metabolites, will require targeted perturbation experiments.

320 The early postnatal cortical signatures observed at P8 likely reflect a combination of
321 processes – altered progenitor behavior, maturation state, survival, or subtype specification – that
322 shift the relative abundance of projection-neuron subtype marker populations. We used SATB2,
323 CTIP2, and TBR1 as operational indices of major projection-neuron subclasses during early
324 postnatal development; future work will be needed to determine whether these differences reflect
325 fate specification versus later developmental remodeling and whether they persist into adulthood.
326 Increased microglial density and astrocytic reactivity in exposed offspring suggest a broader
327 developmental response that may interact with neuronal maturation, but mechanistic relationships
328 among these findings remain to be determined.

329 Behaviorally, prenatal LSD exposure was associated with increased stereotyped rotation
330 and with PPI reductions that were most robust in males after repeated exposure. These outcomes
331 are not specific to any one neurodevelopmental condition, and we therefore interpret them as
332 behavioral readouts consistent with altered circuit function rather than as disease models. Taken

333 together, our data support a temporally coherent model in which rapid embryonic CSF access and
334 ChP activation coincide with downstream cortical and behavioral phenotypes. Because the
335 embryonic ChP assays, P8 histology, and adult behavior were collected in separate cohorts and
336 without receptor/ChP perturbation, we present the ChP→cortex→behavior sequence as a working
337 model rather than a demonstrated causal pathway.

338 Several limitations are important for interpretation. First, we used a single dose level and
339 focused on acute versus repeated exposure regimens, which constrains inferences about dose-
340 response relationships. Second, our dose selection was guided by rodent literature (Halberstadt
341 and Geyer, 2013; Maitland et al., 2025; McGriff et al., 2025) and the need for robust exposure and
342 assay sensitivity in embryonic CSF; it is not intended to model human exposure levels, and we do
343 not attempt to estimate pregnancy risk. Addressing these limitations with PK/PD-anchored dosing,
344 receptor perturbation (e.g. pharmacological antagonism or genetic approaches), and longitudinal
345 anatomical/behavioral mapping will be essential for resolving causal mechanisms.

346 In summary, our data show that maternal LSD can access embryonic CSF on a minutes
347 timescale and that embryonic ChP epithelium mounts a rapid response to serotonergic agonists
348 during cortical development. These findings provide a framework for studying how maternal
349 serotonergic exposures may engage the embryonic CSF-choroid plexus interface and motivate
350 future mechanistic experiments to define receptor pathways and downstream developmental
351 consequences.

352

353

354 **References**

355 Bonnin A, Goeden N, Chen K, Wilson ML, King J, Shih JC, Blakely RD, Deneris ES, Levitt P
356 (2011) A transient placental source of serotonin for the fetal forebrain. Nature:2–7.

357 Carvajal-Oliveros A, Campusano JM (2021) Studying the Contribution of Serotonin to
358 Neurodevelopmental Disorders. Can This Fly? Front Behav Neurosci 14:601449.

359 Courtney Y, Head JP, Dani N, Chechneva OV, Shipley FB, Zhang Y, Holtzman MJ, Sadegh C,
360 Libermann TA, Lehtinen MK (2025) Choroid plexus apocrine secretion shapes CSF
361 proteome during mouse brain development. Nat Neurosci:1–14.

362 Courtney Y, Lehtinen MK (2025) Apocrine secretion by the choroid plexus. Fluids and Barriers
363 of the CNS 22:75.

364 Damkier HH, Brown PD, Praetorius J (2013) Cerebrospinal fluid secretion by the choroid
365 plexus. Physiol Rev 93:1847–1892.

366 Dani N et al. (2021) A cellular and spatial map of the choroid plexus across brain ventricles and
367 ages. Cell 184:3056-3074.e21.

368 Fame RM, Lehtinen MK (2020) Emergence and Developmental Roles of the Cerebrospinal Fluid
369 System. Dev Cell 52:261–275.

370 Gaspar P, Cases O, Maroteaux L (2003) THE DEVELOPMENTAL ROLE OF SEROTONIN :
371 NEWS FROM MOUSE MOLECULAR GENETICS. Nature Reviews Neuroscience 4.

372 Gato A, Desmond ME (2009) Why the embryo still matters: CSF and the neuroepithelium as
373 interdependent regulators of embryonic brain growth, morphogenesis and histiogenesis.
374 Developmental Biology 327:263–272.

375 Halberstadt AL, Geyer MA (2013) Characterization of the head-twitch response induced by
376 hallucinogens in mice: detection of the behavior based on the dynamics of head
377 movement. Psychopharmacology (Berl) 227:10.1007/s00213-013-3006-z.

378 Lehtinen MK, Zappaterra MW, Chen X, Yang YJ, Hill AD, Lun M, Maynard T, Gonzalez D,
379 Kim S, Ye P, D'Ercole AJ, Wong ET, LaMantia AS, Walsh CA (2011) The
380 Cerebrospinal Fluid Provides a Proliferative Niche for Neural Progenitor Cells. Neuron
381 69:893–905.

382 Lun MP, Monuki ES, Lehtinen MK (2015) Development and functions of the choroid plexus-
383 cerebrospinal fluid system. Nature Reviews Neuroscience 16:445–457.

384 MacAulay N, Keep RF, Zeuthen T (2022) Cerebrospinal fluid production by the choroid plexus:
385 a century of barrier research revisited. Fluids Barriers CNS 19:26.

386 Maitland AD, Gonzalez NR, Walther D, Pereira F, Baumann MH, Glatfelter GC (2025) Rapid,
387 Open-Source, and Automated Quantification of the Head Twitch Response in C57BL/6J

388 Mice Using DeepLabCut and Simple Behavioral Analysis. ACS Pharmacol Transl Sci
389 8:2694–2709.

390 McGriff SA, Hecker JC, Maitland AD, Partilla JS, Baumann MH, Glatfelter GC (2025)
391 Psychedelic-like effects induced by 2,5-dimethoxy-4-iodoamphetamine, lysergic acid
392 diethylamide, and psilocybin in male and female C57BL/6J mice. Psychopharmacology
393 Available at: https://doi.org/10.1007/s00213-025-06795-x [Accessed August 17, 2025].

394 Sanders-Bush E, Breeding M (1991) Choroid plexus epithelial cells in primary culture: a model
395 of 5HT1C receptor activation by hallucinogenic drugs. Psychopharmacology (Berl)
396 105:340–346.

397 Saunders NR, Dziegielewska KM, Fame RM, Lehtinen MK, Liddelow SA (2023) The choroid
398 plexus: a missing link in our understanding of brain development and function.
399 Physiological Reviews 103:919–956.

400 Shah R, Courtiol E, Castellanos FX (2018) Abnormal Serotonin Levels During Perinatal
401 Development Lead to Behavioral Deficits in Adulthood. Frontiers in Behavioral
402 Neuroscience 12:1–10.

403 Yagaloff KA, Hartig PR (1985) 125I-lysergic acid diethylamide binds to a novel serotonergic
404 site on rat choroid plexus epithelial cells. J Neurosci 5:3178–3183.

405 Zappaterra MW, LaMantia AS, Walsh CA, Lehtinen MK (2013) Isolation of Cerebrospinal Fluid
406 from Rodent Embryos for use with Dissected Cerebral Cortical Explants. J Vis
407 Exp:50333.

408

409 **Acknowledgments:** We thank the NIDA Drug Supply Program for providing controlled
410 substances (LSD, psilocybin, and 5-MeO-DMT) used in this study. We are grateful to Chinfei
411 Chen, Hisashi Umemori, and Harry Cramer for imaging advice and support, and to the BCH
412 IDDRC Cellular Imaging Core (RRID: SCR_026485) for confocal and light sheet imaging. We
413 are especially grateful to the Boston Children's Hospital Research Controlled Substances Team
414 for their guidance throughout this project. We thank Nathaniel Hodgson and the BCH Animal
415 Behavior and Physiology Core for assistance with behavioral assays. We thank Sofia Bennetts and
416 Pura Arroyo for technical support and help with figures. We are grateful to syGlass (SyGlass, Inc.)
417 for extended access to their visualization software under a trial license and for technical assistance.
418 syGlass had no role in study design, data collection, data analysis, or the decision to publish.

419 Figures were created in part using BioRender.com. We thank members of the Lehtinen lab for
420 valuable feedback and discussions. This work was supported by the National Institutes of Health
421 (R01NS088566 to M.K.L.; P50HD105351 and S10OD030322 to the BCH IDDRC), the Howard
422 Hughes Medical Institute Gilliam Fellowship (Y.C.), the Jane Coffin Childs Memorial Fund for
423 Medical Research Fellowship (Y.C.), and the Kirby Innovation Award (M.K.L.).

424 **Author contributions:**

425 Conceptualization: YC.

426 Methodology: YC, JMA.

427 Investigation: YC, JMA, CLL.

428 Visualization: YC, JMA.

429 Funding acquisition: YC, CJW, MKL.

430 Project administration: CJW, MKL.

431 Supervision: CJW, MKL.

432 Writing – original draft: YC.

433 Writing – review & editing: YC, JMA, CLL, CJW, MKL.

434 **Conflict of Interest:** Authors declare that they have no competing interests.

435 **Data and materials availability:** All data needed to evaluate the conclusions of this study are
436 present in the paper and/or the Supplementary Materials. Additional data and analysis scripts
437 are available from the corresponding author upon reasonable request. Controlled substances
438 (LSD, psilocybin, 5-MeO-DMT) were obtained from the NIDA Drug Supply Program and
439 cannot be redistributed; qualified investigators should request these materials directly from
440 NIDA.

441

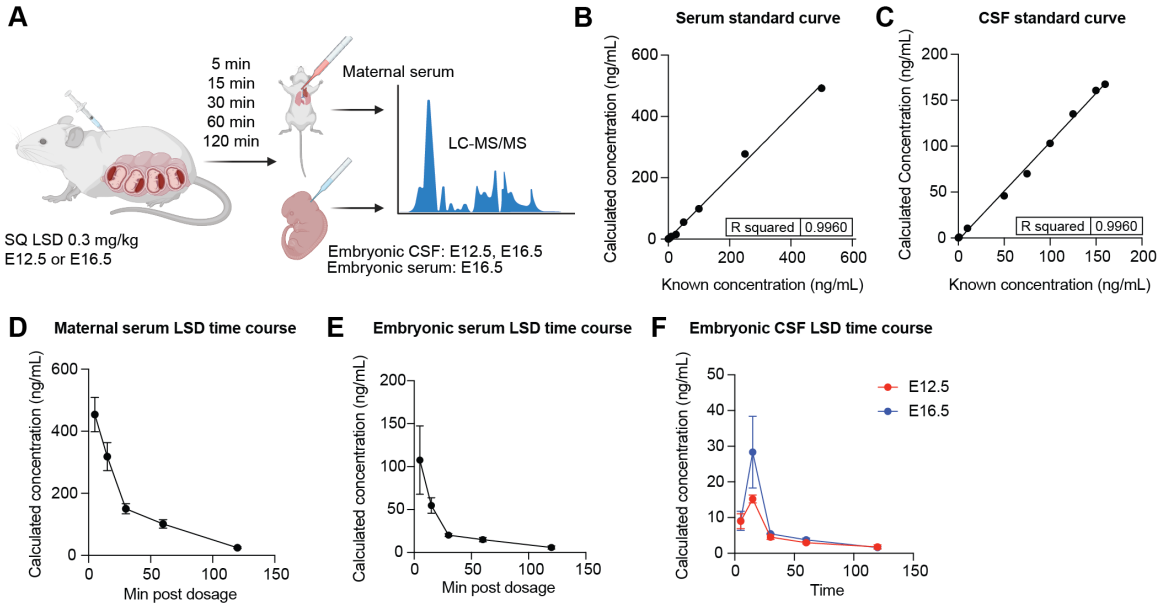

Fig. 1. Maternal LSD rapidly enters embryonic circulation and CSF. (A) Schematic of the pharmacokinetic study. Pregnant mice received a single subcutaneous injection of LSD (0.3 mg kg^{-1}) at E12 .5 or E16.5. Maternal serum, embryonic serum (E16.5) and embryonic CSF (E12.5, E16.5) were sampled at 5, 15, 30, 60, and 120 min and analyzed by LC-MS/MS. **(B)** Calibration curve for LSD spiked into serum ($R^2 = 0.996$). **(C)** Calibration curve for LSD spiked into CSF ($R^2 = 0.996$). **(D)** Time course of LSD concentration in maternal serum after 0.3 mg kg^{-1} LSD (mean ± SEM, n = 3 dams per time point). **(E)** Time course of LSD concentration in E16.5 serum after 0.3 mg kg^{-1} maternal LSD (mean ± SEM, n = 3 pooled litters per time point). **(F)** LSD concentration in embryonic CSF at E12 .5 or E16.5 peaks at 15 min then declines yet remains detectable at 120 min (mean ± SEM, n = 3 pooled litters per time point).

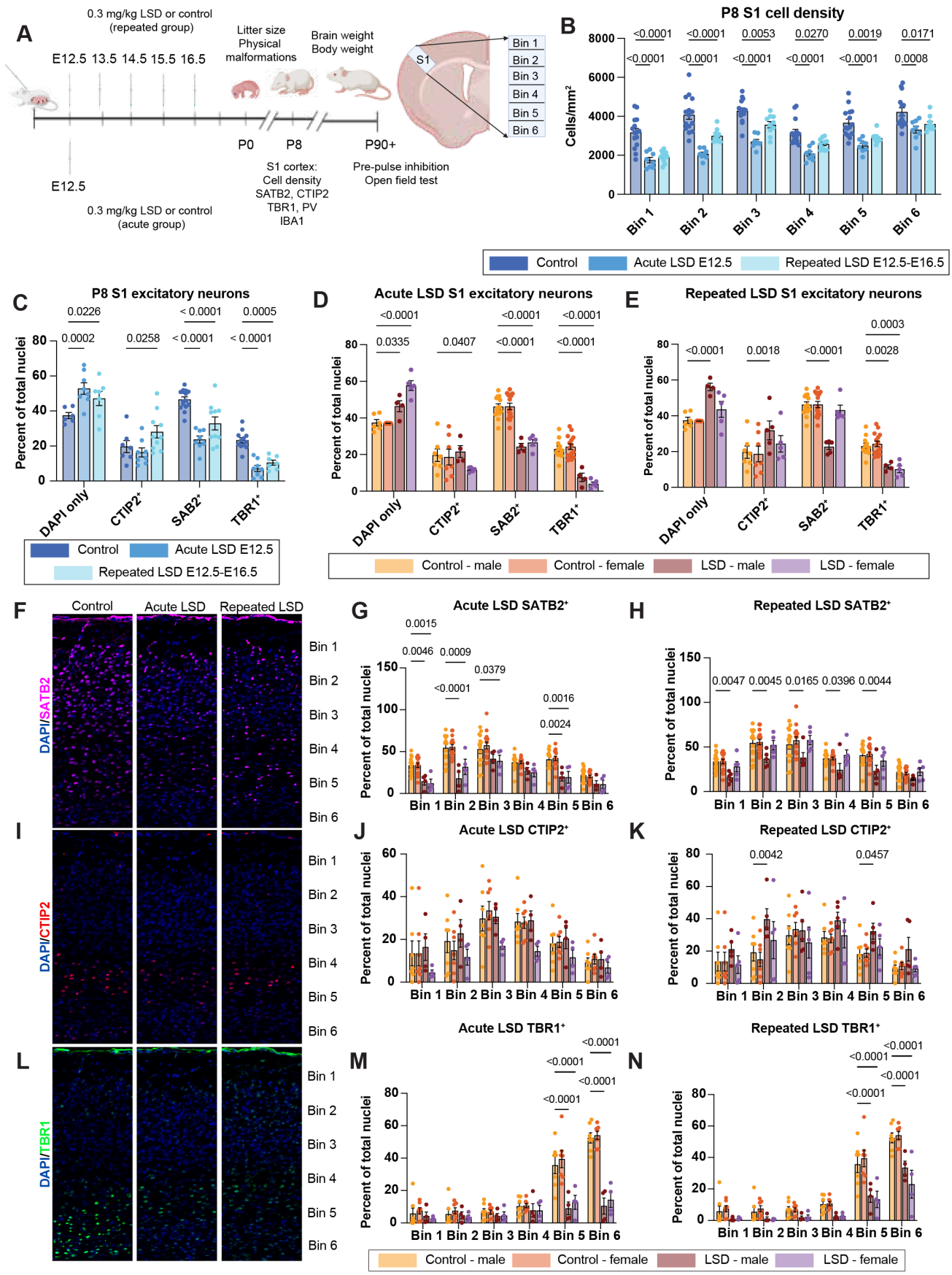
A
0.3 mg/kg LSD or control (repeated group)
E12.5 13.5 14.5 15.5 16.5
Litter size
Physical malformations
Brain weight
Body weight
P0
P8
P90+
E12.5
0.3 mg/kg LSD or control (acute group)
S1 cortex: Cell density SATB2, CTIP2 TBR1, PV IBA1
Pre-pulse inhibition Open field test
S1
Bin 1
Bin 2
Bin 3
Bin 4
Bin 5
Bin 6
B
P8 S1 cell density
Cells/mm²
Control
Acute LSD E12.5
Repeated LSD E12.5-E16.5
C
P8 S1 excitatory neurons
Percent of total nuclei
DAPI only
CTIP2⁺
SAB2⁺
TBR1⁺
D
Acute LSD S1 excitatory neurons
E
Repeated LSD S1 excitatory neurons
Control - male
Control - female
LSD - male
LSD - female
F
Control
Acute LSD
Repeated LSD
DAPI/SATB2
G
Acute LSD SATB2⁺
H
Repeated LSD SATB2⁺
I
DAPI/CTIP2
J
Acute LSD CTIP2⁺
K
Repeated LSD CTIP2⁺
L
DAPI/TBR1
M
Acute LSD TBR1⁺
N
Repeated LSD TBR1⁺

454

455 **Fig. 2. Prenatal LSD alters S1 cortical composition with regimen-dependent and partly sex-**
456 **dependent effects. (A)** Experimental design and S1 sampling. Pregnant dams received a single
457 LSD dose at E12.5 ("acute") or daily doses at E12.5–E16.5 ("repeated") at 0.3 mg kg^{-1}. Brains
458 were analyzed at P8. S1 was divided into six equal-width bins from pia (Bin 1) to white matter
459 (Bin 6). **(B)** Total cell density ($DAPI^+$ nuclei mm^{-2}) across depth. Both regimens reduce nuclei
460 relative to controls; exact post hoc *P* values are printed above bins. **(C)** Sexes pooled: composition
461 of glutamatergic projection-neuron subtype markers expressed as percent of total nuclei (DAPI-
462 only, $CTIP2^+$, $SATB2^+$, $TBR1^+$). Repeated exposure increases $CTIP2^+$ and decreases
463 $SATB2^+/TBR1^+$; acute exposure decreases $SATB2^+/TBR1^+$ without increasing $CTIP2^+$ (panel *P*
464 values shown). For panels **2B-C**, control n = 15 from 3 litters; Acute LSD n = 9 from 3 litters;
465 Repeated LSD n = 10 from 3 litters. **(D–E)** Sex-stratified marker composition for acute (**D**) and
466 repeated (**E**) exposure (color key indicates sex and treatment). **(F)** Representative S1 micrographs
467 (male) stained for SATB2 (green) with DAPI (blue). Scale bar, 50 µm. **(G–H)** $SATB2^+$ neurons
468 by depth after acute (**G**) or repeated (**H**) exposure (percent of total nuclei per bin). Male-biased
469 reductions are evident across superficial to mid layers; bin-wise *P* values are printed. **(I)**
470 Representative S1 micrographs (male) stained for CTIP2 (green) with DAPI (blue). Scale bar, 50
471 µm. **(J–K)** $CTIP2^+$ neurons by depth after acute (**J**) or repeated (**K**) exposure. Repeated exposure
472 produces bin-restricted increases in males (bin-wise *P* values shown). **(L)** Representative S1
473 micrographs (male) stained for TBR1 (green) with DAPI (blue). Scale bar, 50 µm. **(M–N)** $TBR1^+$
474 neurons by depth after acute (**M**) or repeated (**N**) exposure, showing deep-layer losses in both
475 sexes (bin-wise *P* values shown). For panels 2**D-N**, control male n = 7 from 3 litters, control female
476 n = 7 from 3 litters, acute LSD male = 4 from 3 litters, acute LSD female n = 5 from 3 litters,
477 repeated LSD male n = 5 from 3 litters, repeated LSD female n = 5 from 3 litters.
478

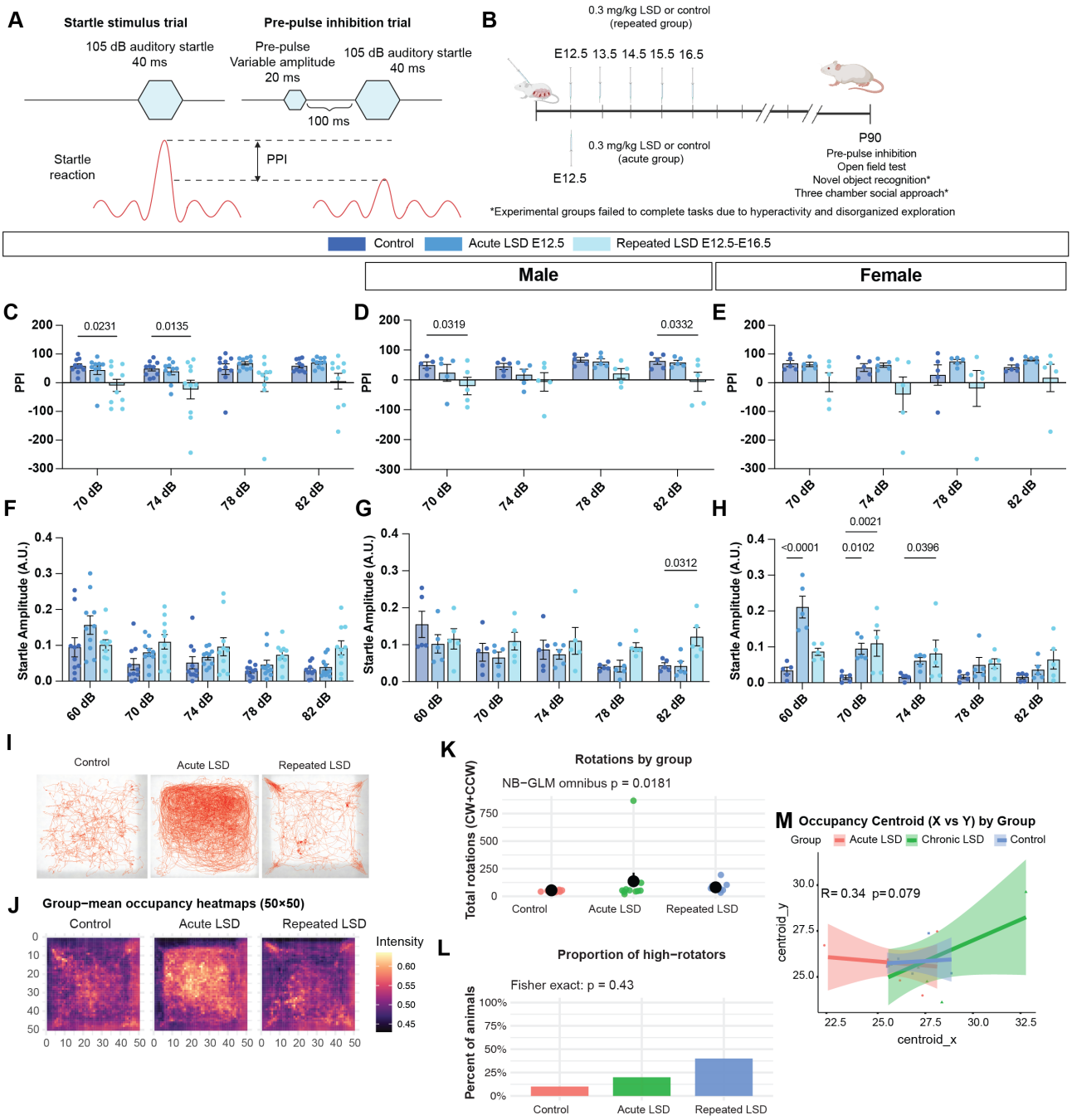
A
Startle stimulus trial
Pre-pulse inhibition trial
105 dB auditory startle
40 ms
Pre-pulse
Variable amplitude
20 ms
105 dB auditory startle
40 ms
100 ms
Startle
reaction
PPI
B
0.3 mg/kg LSD or control
(repeated group)
E12.5 13.5 14.5 15.5 16.5
0.3 mg/kg LSD or control
(acute group)
E12.5
P90
Pre-pulse inhibition
Open field test
Novel object recognition*
Three chamber social approach*
*Experimental groups failed to complete tasks due to hyperactivity and disorganized exploration
Control
Acute LSD E12.5
Repeated LSD E12.5-E16.5
Male
Female
C
D
E
PPI
0.0231
0.0135
0.0319
0.0332
70 dB
74 dB
78 dB
82 dB
F
G
H
Startle Amplitude (A.U.)
<0.0001
0.0021
0.0102
0.0396
0.0312
60 dB
70 dB
74 dB
78 dB
82 dB
I
Control
Acute LSD
Repeated LSD
J
Group−mean occupancy heatmaps (50×50)
Control
Acute LSD
Repeated LSD
Intensity
K
Rotations by group
NB−GLM omnibus p = 0.0181
Total rotations (CW+CCW)
Control
Acute LSD
Repeated LSD
L
Proportion of high−rotators
Fisher exact: p = 0.43
Percent of animals
M
Occupancy Centroid (X vs Y) by Group
Group
Acute LSD
Chronic LSD
Control
R= 0.34 p=0.079
centroid_y
centroid_x

482 **Fig. 3. Embryonic LSD exposure reduces prepulse inhibition and increases rotational**
483 **stereotypy.** Analyses were blinded; litter was tracked and included as a random intercept in
484 sensitivity models. For all behavioral assays presented, control n = 10 from 3 litters, acute LSD n
485 = 10 from 3 litters, repeated LSD n = 10 from 3 litters; 5 male and 5 female mice per experimental
486 condition. **(A)** PPI task schematic. **(B)** Maternal dosing and testing timeline (acute E12.5; repeated
487 E12.5–E16.5; saline controls). **(C–E)** Prepulse inhibition (PPI) at P90: **(C)** sexes pooled, PPI
488 reduced after prenatal LSD; **(D)** males, reduced PPI after repeated exposure; **(E)** females, no
489 group-level difference at this N despite individual variability. **(F–H)** Startle amplitude across
490 intensities (A.U.): **(F)** sexes pooled; **(G)** males, higher amplitude only for the repeated group at 82
491 dB; **(H)** females, higher amplitude in several LSD conditions across intensities. **(I)** Open-field
492 examples: single-animal path traces. **(J)** Group-mean occupancy heatmaps (50×50 grid). **(K)** Total
493 rotations by group (negative-binomial GLM, omnibus $\chi^2 = 8.02$, P = 0.018); back-transformed
494 means ± SE: Control 54.2 ± 12.6, Acute 136.2 ± 31.3, Repeated 81.4 ± 18.8; Tukey Control vs
495 Acute P = 0.013. **(L)** Proportion of "high-rotators" (threshold = 95th percentile of Control; Fisher
496 exact P = 0.43; n/N shown). **(M)** Occupancy centroids (x by y), sexes pooled; lines show group-
497 wise linear fits with 95% confidence bands (R = 0.34, P = 0.079).

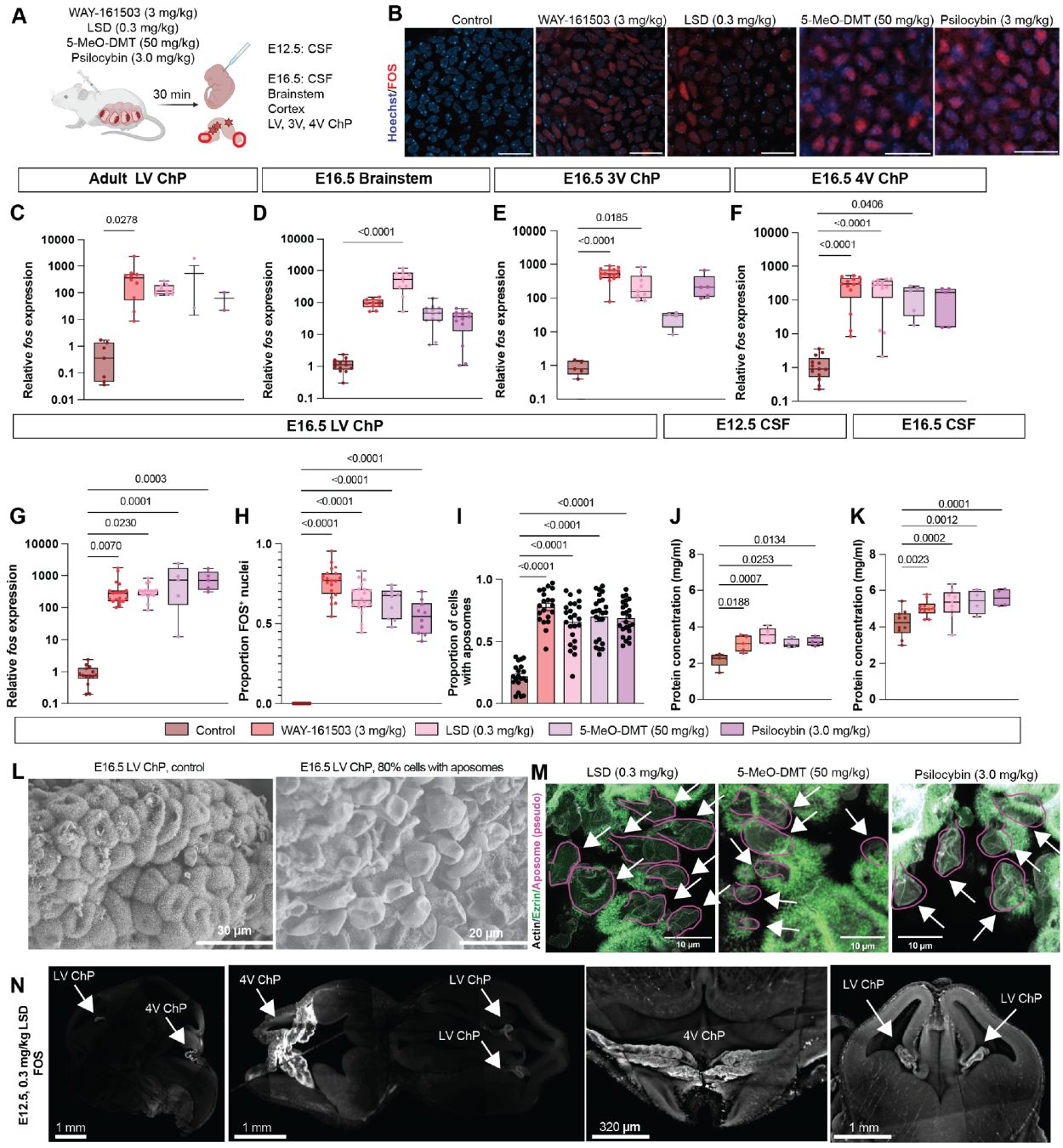
A
WAY-161503 (3 mg/kg)
LSD (0.3 mg/kg)
5-MeO-DMT (50 mg/kg)
Psilocybin (3.0 mg/kg)
30 min
E12.5: CSF
E16.5: CSF
Brainstem
Cortex
LV, 3V, 4V ChP
B
Control
WAY-161503 (3 mg/kg)
LSD (0.3 mg/kg)
5-MeO-DMT (50 mg/kg)
Psilocybin (3 mg/kg)
Hoechst/FOS
Adult LV ChP
E16.5 Brainstem
E16.5 3V ChP
E16.5 4V ChP
C
D
E
F
Relative fos expression
E16.5 LV ChP
E12.5 CSF
E16.5 CSF
G
H
I
J
K
Proportion FOS+ nuclei
Proportion of cells with aposomes
Protein concentration (mg/ml)
Control
WAY-161503 (3 mg/kg)
LSD (0.3 mg/kg)
5-MeO-DMT (50 mg/kg)
Psilocybin (3.0 mg/kg)
L
E16.5 LV ChP, control
E16.5 LV ChP, 80% cells with aposomes
30 µm
20 µm
M
LSD (0.3 mg/kg)
5-MeO-DMT (50 mg/kg)
Psilocybin (3.0 mg/kg)
Actin/Ezrin/Aposome (pseudo)
10 µm
N
E12.5, 0.3 mg/kg LSD
FOS
LV ChP
4V ChP
1 mm
320 µm

498

499

500 **Fig. 4. Maternal serotonergic agonists rapidly activate embryonic choroid plexus and**
501 **increase embryonic CSF protein. (A)** Experimental design: pregnant dams dosed at E12.5 (LSD
502 0.3 mg kg^{-1}; 5-MeO-DMT 50 mg kg^{-1}; psilocybin 3 mg kg^{-1}; WAY-161503 3 mg kg^{-1}); tissues
503 and CSF collected 30 min later. Additional cohorts at E16.5 as indicated. **(B)** c-FOS
504 immunostaining in ChP epithelium 30 min post-dose (representative fields; Hoechst/c-FOS). **(C)**
505 Dam LV ChP: *Fos* expression (qPCR; 2^-ΔΔCt; normalized to *18s,* relative to vehicle). Control n
506 = 7 ChP tissues, WAY n = 10, LSD n = 10, 5-MeO-DMT n = 2, psilocybin n = 2. **(D–F)** E16.5
507 ChP/brainstem: relative *Fos* expression in **D**, brainstem (Control n = 13 ChP tissues from 3 litters,
508 WAY n = 10 from 3 litters, LSD n = 10 from 3 litters, 5-MeO-DMT n = 13 from 3 litters, psilocybin
509 n = 13 from 3 litters); **E**, 3V ChP (Control n = 5 ChP tissues from 3 litters, WAY n = 15 from 3
510 litters, LSD n = 9 from 3 litters, 5-MeO-DMT n = 4 from 3 litters, psilocybin n = 5 from 3 litters);
511 **F**, 4V ChP (Control n = 13 ChP tissues from 3 litters, WAY n = 13 from 3 litters, LSD n = 13 from
512 3 litters, 5-MeO-DMT n = 5 from 3 litters, psilocybin n = 5 from 3 litters). **(G)** E16.5 LV ChP:
513 relative *Fos* expression (Control n = 14 ChP tissues from 3 litters, WAY n = 20 from 3 litters, LSD
514 n = 17 from 3 litters, 5-MeO-DMT n = 5 from 3 litters, psilocybin n = 5 from 3 litters). **(H)**
515 Proportion of FOS^+ nuclei in E16.5 4V ChP (image-based quantification; control n = 13 ChP
516 tissues from 3 litters, WAY n = 20 from 3 litters, LSD n = 20 from 3 litters, 5-MeO-DMT n = 10
517 from 3 litters, psilocybin n = 10 from 3 litters). **(I)** Proportion of ChP epithelial cells with apocrine
518 blebs at 30 min (control n = 20 ChP tissues from 3 litters, WAY n = 20 from 3 litters, LSD n = 24
519 from 3 litters, 5-MeO-DMT n = 24 from 3 litters, psilocybin n = 24 from 3 litters). **(J–K)** Total
520 protein concentration in embryonic CSF: **J**, E12.5 (control n = 5 pooled litters, WAY n = 5 pooled
521 litters, LSD n = 5 pooled litters, 5-MeO-DMT n = 4 pooled litters, psilocybin n = 4 pooled litters);
522 **K**, E16.5 (control n = 10 pooled litters, WAY n = 10 pooled litters, LSD n = 9 pooled litters, 5-
523 MeO-DMT n = 4 pooled litters, psilocybin n = 4 pooled litters). (**L**) SEM of E16.5 LV choroid

524 plexus comparing baseline aposome formation (left) with a high-frequency state (right; ~80%
525 aposome-positive epithelial cells). (**M**) High-resolution confocal images of E16.5 ChP epithelium
526 30 min after LSD, 5-MeO-DMT, or psilocybin exposure shows extensive apical blebbing and
527 redistribution of actin and ezrin, a marker of microvilli and membrane curvature. **(N)** Light-sheet
528 fluorescence imaging of optically cleared E12.5 heads stained for c-FOS 30 min post maternal 0.3
529 mg kg^{-1} LSD (representative embryo). Cross-sections of whole-head dataset highlight strong
530 activation in 4V ChP and detectable signal in LV ChP (arrows). Scattered bright foci are non-
531 cellular artifacts (e.g., vascular-associated antibody retention and secondary antibody pooling)
532 characteristic of this non-perfused, whole-embryo staining method. Scale bars as indicated.